

SYNTHESIS AND CHARACTERISATION OF COPPER NANOPARTICLES BY DIFFERENT METHODS

FANCY SUJIMALAR

Research Scholar
M.Phil Chemistry
Bharath Institute Of Higher Education And Research
Mail Id : fancyrobsonirin@gmail.com

Mrs. E. REKHA

Assistant Professor, Department of Chemistry
Bharath Institute of Higher Education And Research

Address for Correspondence:

FANCY SUJIMALAR

Research Scholar
M.Phil Chemistry
Bharath Institute Of Higher Education And Research
Mail Id : fancyrobsonirin@gmail.com

ABSTRACT

Nano ferrites, particularly spinel ferrites, have attracted more attention in recent years due to their technological applications. By incorporating suitable divalent, trivalent or tetravalent impurities into the spinel lattice, the properties of nano ferrites could be tailored. Particle size plays a key role in the magnetic behaviour of materials as well as in biomedical applications. They can be used in biomedical applications by manipulating particle size, shape and magnetic behaviour.

Sol gel method was primarily used in the preparation of $\text{Cu}_{1-x}\text{Ni}_x\text{Fe}_2\text{O}_4$ ($x= 0, 0.5, 1$) nanoparticles in this study among the synthesis methods. In the synthesis process, iron nitrate and nickel, copper ferrite were used as oxidizers and green reducing agent was used as fuel. For the synthesis of $\text{Cu}_{1-x}\text{Ni}_x\text{Fe}_2\text{O}_4$ ($x= 0, 0.5, 1$) green reducing agents such as honey, aloe vera extract, egg white, lemon juice and sugarcane juice were used and the resulting property changes were analyzed.

In CuFe_2O_4 nanoparticles, nickel (Ni^{2+}) ions are substituted by Fe^{3+} ions. Particle size, surface morphology and magnetic behaviour were studied in CuFe_2O_4 nanoparticles by substituting the Ni^{2+} ions instead of Fe^{3+} ions.

Different techniques such as X-ray diffraction, FTIR spectroscopy, Scanning Electron Microscopy, Transmission Electron Microscopy, Energy Dispersive X-ray Spectroscopy and magnetic properties were used to characterize the synthesized nano ferrite samples using Vibrating Sample Magnetometry (VSM). Nickel substitution was found to decrease the particle size of copper ferrite for all processes based on green reducing agents. Aloe Vera extract based combustion gave better result compared to other green fuels. $\text{Cu}_{1-x}\text{Ni}_x\text{Fe}_2\text{O}_4$ nanoparticles prepared by using aloe vera extract as a fuel has some unique properties, For example it has less particle size , more of energy band gap , better other fuels. The absorption band vibration spectra showed the metal-oxide vibrating band (M-O) and it was shown that the metal ion together with oxygen occupied in tetrahedral and octahedral sites were observed as 407 ± 5 and 523 ± 5 cm^{-1} for the prepared ferrite nanoparticles. Due to the combustion effect, remarkable changes were observed in the surface morphology by changing the fuel. The energy bandgap values as 1.78 eV using the UV-Vis absorbance spectrum. Saturation magnetization was observed to increase by adding nickel to all processes based on green fuel, but the process based on sugarcane juice significantly decreases the value of saturation magnetization. Variations in structural and magnetic parameters may be due to changes in the complexion, strength, reducing power, the content of the evolution of the gas, the reaction rate, the enthalpy, etc. of the reducing agents.

INTRODUCTION

INTRODUCTION

Humans have always been in search of materials for potential applications to satisfy their need and greed. Investigation of new materials with enhanced properties initiated a careful study of the synthesis, processing, and characterization of materials. Nowadays, magnetic materials are becoming more essential in modern-technology electronic devices, in industrial equipment and in medical equipment. The word ‘magnetism’ was first associated with a mineral called magnetite (Fe_3O_4). The attracting power of magnetic materials toward the iron was identified around 2500 years ago. But its power of attracting iron was certainly known for centuries before Christ. In fact, nearly everything known about the magnetic properties of materials was derived from experimental discoveries and a few were based on assumptions.

Derived from the Latin word ‘Ferrum’, the term *ferrite* refers to the main element of mixed metal oxide ($\text{MO.Fe}_2\text{O}_3$) with ferric oxide (Fe_2O_3). The high technological significance of ferrites in the contemporary electronic industry may be due to their importance as a magnetic material. Because of their high production, ferrites have been reported parameters of the ferrites can also be modified/improved by a small quantity of foreign metal ions as dopants (Gupta *et al.* 2012). At the moment, there has been both interest and nanoferrites as far better than those of pure ferrite materials. Nanoferrite particles demonstrate novel magnetic characteristics that are not common to their bulk counterparts such as single-domain behaviour and superparamagnetism. Ferrites are used in ferrofluids, ferroseals, solar energy devices, radar, satellite communications systems, microwave devices, computer memory and audio-video digital recordings and as permanent magnets.

clinical and biomedical application, because of their size in the nano-region, biocompatibility, porous nature and also their magnetic behaviour (Gee *et*

Research Paper

al. 2003). Biomedical applications are restricted to the requirements from the nanomaterials' behaviour such as chemical stability, composition, size, homogeneous distribution, crystal structure, magnetic parameters, high surface area, biocompatibility, solubility, less toxicity level, and non-allergic system (Sun *et al.* 2002).

MAGNETIC DOMAINS

The theory of domain describes the magnetization and hysteresis of ferromagnetic materials. Ferromagnets comprise a number of tiny areas known as domains. In ferromagnetic domains all magnetic dipoles are aligned parallel to each other and each domain is oriented toward the other to cancel the stray fields. The sample shape determines the domain size. If a ferromagnetic material is in its demagnetized state, the average magnetization is zero. Domains are divided by walls of the domain. Domain formation allows minimizing the complete materials. The primary contribution to magnetic energy is, magnetocrystalline energy, and magnetostrictive energy.

PROPERTIES OF MAGNETIC MATERIALS**Magnetic Anisotropy**

Magnetic anisotropy usually relates to magnetic characteristics based on the direction of measurement. The magnitude and type of magnetic anisotropy in magnetic materials influence the characteristics such as magnetization curves and hysteresis.

VARIATION OF COERCIVITY WITH PARTICLE SIZE INFINE PARTICLES

Magnetic behaviour of domains depends largely on the particle size or diameter. On the basis of the particle diameter, magnetic behaviour is divided into four types, as shown in Figure 1.3

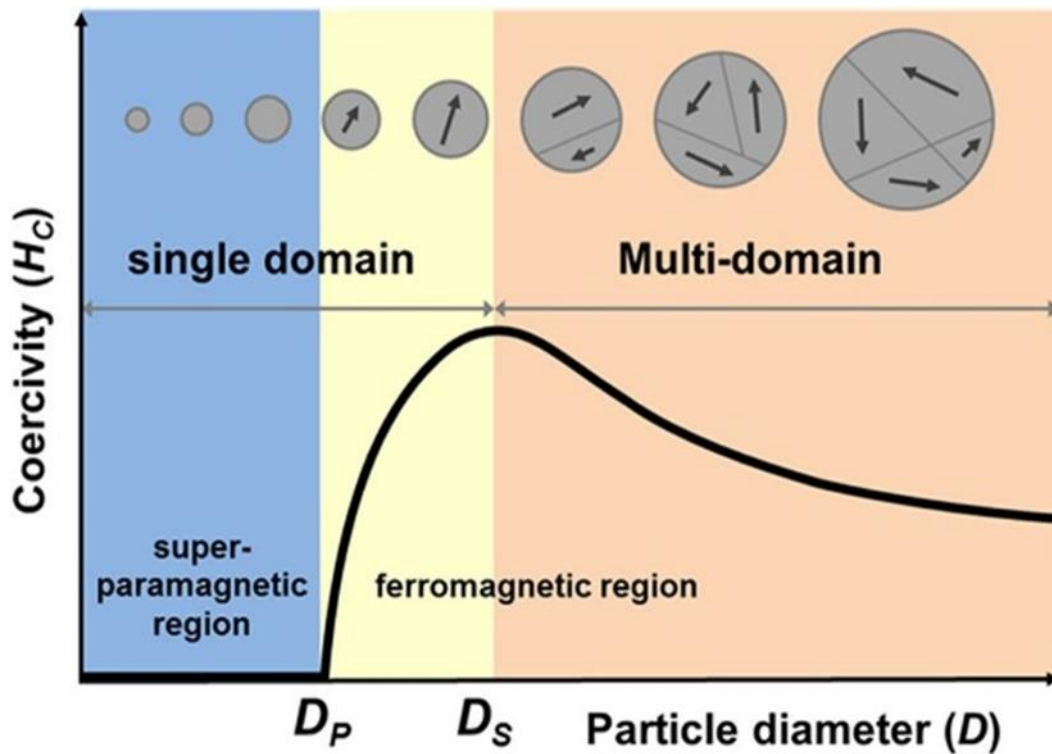


Figure 1.3 Schematic of the variation in coercivity with particle diameter (Source: Lee *et al.* 2015).

If there is a single domain of a large magnetic material, the surface energy due to magnetic dipoles will be opposed to the intrinsic magnetism, resulting in large magnetostatic surface energy. It is the intrinsic tendency of any material to remain in a stable minimum state of energy. Therefore, the large magnetic material breaks down into tiny regions called domains to minimize their energy. This splitting into smaller and smaller domains will proceed until the equilibrium of domains is reached for a given particle size. Thus, neighboring domains will have distinct magnetization directions and the exchange and magnetocrystalline energy will decide the size and strength of domain walls.

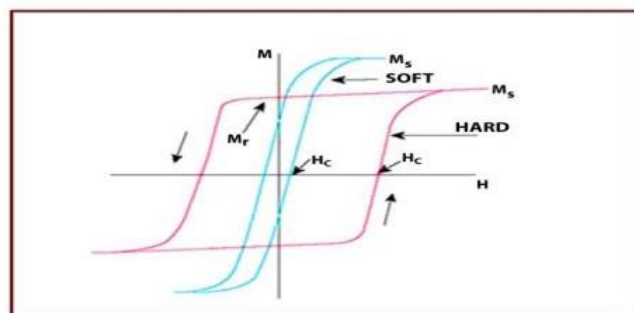


Figure 1.4 Typical magnetic hysteresis

AIM OF THE PRESENT WORK

One of the aims of this investigation is to synthesize $\text{Cu}_{1-x}\text{Ni}_x\text{Fe}_2\text{O}_4$ nanoparticles using a simple, economical and green combustion method. It becomes evident after the literature survey that $\text{Cu}_{1-x}\text{Ni}_x\text{Fe}_2\text{O}_4$ nanoparticles were extensively studied because of interest in their magnetic properties. The physical and temperature annealing and distribution of time and cation at different sites. The samples were prepared using the sol–gel method. The other methods require complex and costly synthesis equipment. The method of green combustion is easier and cheaper. It also ensures proper metal mixing and homogeneity in the synthesized sample. Also, the particles obtained using this method is smaller. In this thesis, the ferrites studied are CuFe_2O_4 , $\text{Cu}_{0.5}\text{Ni}_{0.5}\text{Fe}_2\text{O}_4$ and NiFe_2O_4 nanoparticles. Use of five green reducing agents such as aloe vera extract, honey, egg white, lemon juice and sugar cane juice is studied.

EXPERIMENTAL TECHNIQUES

INTRODUCTION

Ferrite nanomaterials are of technical and scientific interest due to their typical optical, magnetic and electrical properties. Magnetic nanoparticles are used in the field of bio magnetics for a wide range of applications, such as drug delivery and sensing. The nonconventional techniques of bottom-up nanotechnology, particularly sol–gel technique, enable the preparation of highly reactive ferrite nanoparticles. The composition, microstructure, size and characteristics can be rigorously monitored to meet the specific demands of multiple sophisticated applications. This chapter deals with the ferrite synthesis technique and also provides an insight into the instrumentation details of the different characterization techniques .

SYNTHESIS OF NANOMATERIALS

Top-down routes are based on the bulk material and make it smaller by using physical procedures such as crushing, milling or grinding to break up bigger particles. This route is not appropriate for the preparation of uniformly developed materials with high energy consumption.

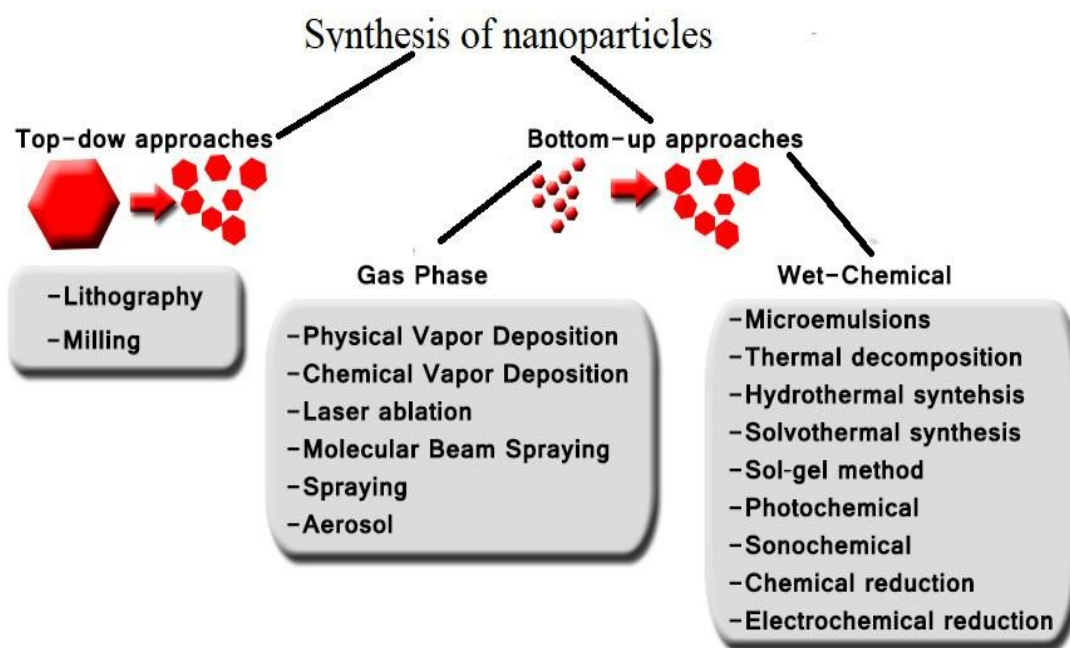


Figure 2.1 Synthesis method of nanoparticles

Sol-gel Method

Sol-gel processing, a little more than the standard solution chemistry, is useful because of its easy operation. In this technique, the initial objective is to produce that is a in liquid of colloidal particle. The colloidal particles may or may not have the required the chemical structure of the end product. The particles are eventually connected to form a gel through the attraction of van der Waal force with elevated porosity and specific surface area. If the target material is a nanoscale powder, the gel can be dried and grounded simply. This route can also be used to produce carbides, nitrides, and sulfides.

The sol-gel process characterized distinctstep (Hamid *et al.* 2003,

Research Paper

Segal *et al.* 1997). These are:

Sol–Gel process advantages

- Better homogeneity
- Preparation at low temperature, saving energy
- Less losses of evaporation
- Less air pollution

Sol–gel process disadvantages

- Compared to mineral-based metal ion sources, raw materials for this method are costly (in the case of metal alcoxides).

Hydrothermal Method

In hydrothermal synthesis, water is used efficiently to prepare fine powders of metal oxide nanoparticles. Water performs two significant roles for the precursors under these hydrothermal circumstances: a stress transmitting medium and a solvent. Such circumstances will decrease the activation energy for the final phase formation, which can also accelerate the precursor response; An autoclave is invariably used for this process (Carp *et al.* 2004).

GREEN SYNTHESIS AND CHARACTERIZATIONS OF HONEY-MEDIATED NICKEL-COPPER-MIXED FERRITE NANOPARTICLES

INTRODUCTION

With the discovery of mixed ferrites, a fascinating universe of ceramic products arose as a promising study area (Gupta *et al.* 2013). A study conducted over the last few decades has revealed high formation facilities, lower cost, greater efficiency and unique magnetic properties. Therefore, mixed ferrite has extensive tools, ferrofluids, sensors, and magnetic medicine carriers (Kaur *et al.* 2012, Watawe *et al.* 2007). The synthesis of spinel ferrites using methods such as

Research Paper

ceramics, coprecipitation, hydrothermal and many other approaches has been reported.

In this study, pure and Cu-Ni-mixed ferrite nanoparticles were reducing agent in the method adopted includes homogeneous mixing of literature (Tehrani *et al.* 2012, Anjana *et al.* 2018, Mahalakshmi *et al.* 2015).

This study lists chemicals and experimental procedures used for the synthesis of $\text{Cu}_{1-x}\text{Ni}_x\text{Fe}_2\text{O}_4$ ($x = 0, 0.5, 1.0$) ferrite nanoparticles using fresh honey by sol–gel technique. It also presents the results and discussion part of synthesized ferrite nanoparticles. The subsequent sections of this chapter deal about a variety of analytical tools that have been used to validate the nanoparticles.

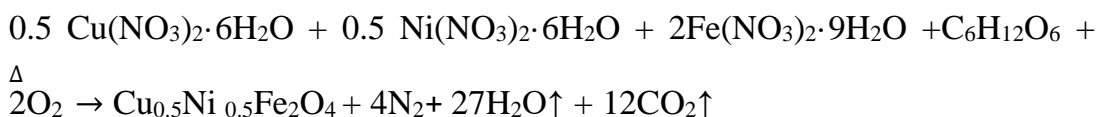
HONEY-MEDIATED NICKEL-COPPER-MIXED FERRITE NANOPARTICLES BY SOL–GEL METHOD

Chemicals Used

Various chemicals used for synthesis were analytical-grade copper $[\text{Fe}(\text{NO}_3)_2 \cdot 9\text{H}_2\text{O}]$ with purity ranging from 98% to 99%. Pure honey (Dabur India Pvt Ltd) was obtained from a nearby local market.

Experimental Procedure

The following equation shows rottenness of metal–honey ferrite gel precursor to Cu-Ni ferrite nanoparticles:



Research Paper

Then, the prepared nanoparticles were tested by using several strategies.

The synthesized copper ferrite, copper-nickel mixed ferrite, nickel ferrite samples were denoted as CuF, CuNiF, and NiF, respectively.

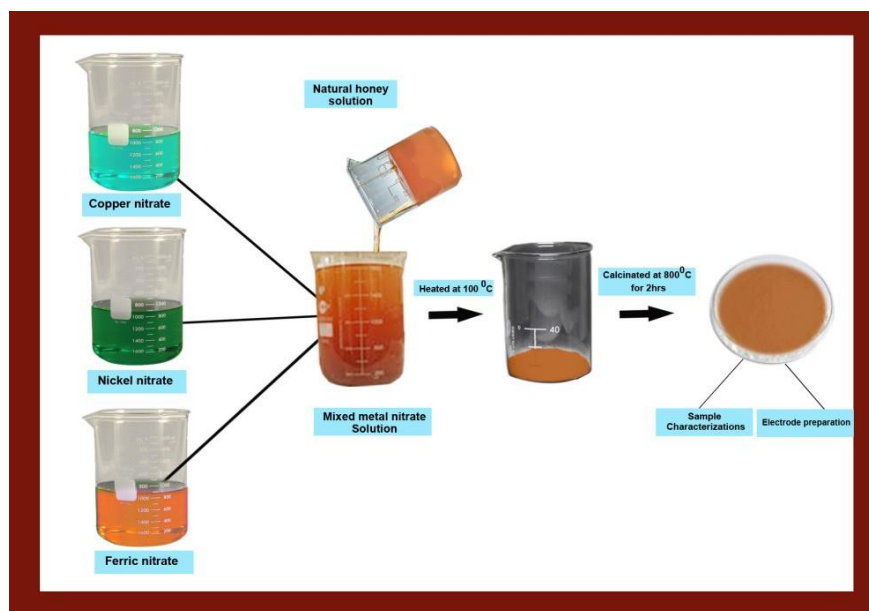


Figure 3.1 Synthesis of honey-mediated Cu-Ni ferrite nanoparticles

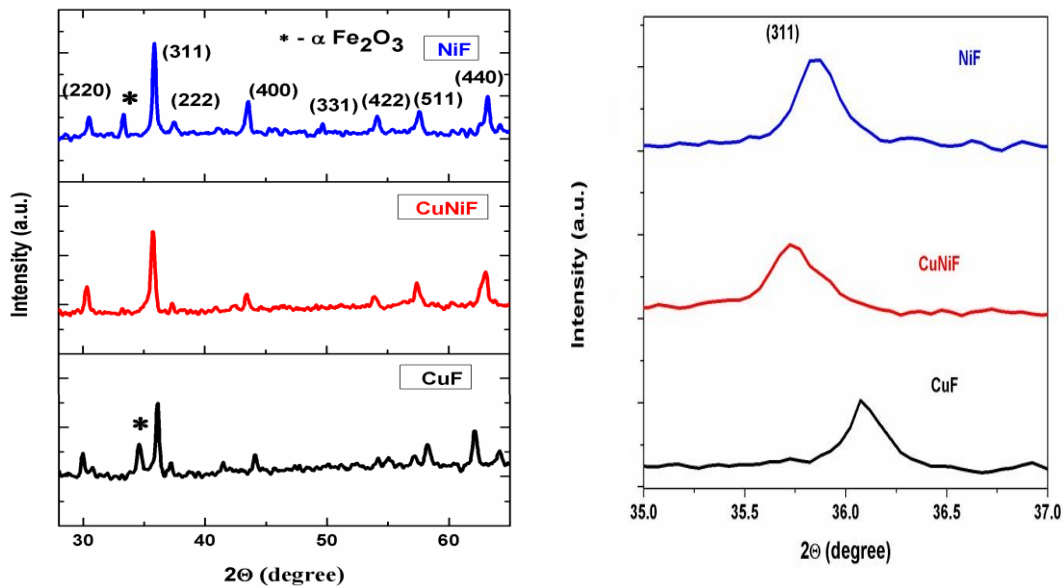
RESULTS AND DISCUSSION

Structural Analysis

Powder XRD analysis

XRD measurements were performed to identify the crystallographic structure and to estimate the size of the crystallite. Figure 3.2 shows the XRD pattern of honey-mediated $\text{Cu}_{1-x}\text{Ni}_x\text{Fe}_2\text{O}_4$ ($x = 0.0, 0.5, 1.0$) nanoparticles. The XRD diffraction peak appears at the planes of (220), (311), (222), (400), (422), (511), and (440). It reveals that the prepared materials exhibit spinel phase diffraction reflections with a cubic spinel structure that are well matched with JCPDS File Card No. 77-0010 for copper ferrite (Chatterjee *et al.* 2014) and JCPDS Card No. 10-0325 for nickel ferrite (Sivakumar *et al.* 2011). Minor secondary-phase reflections peaks corresponding to Fe_2O_3 were observed for the CuF and NiF samples.

Major peaks (220), (311), (400), and (440) are present in all samples. Addition of Ni²⁺ content to CuF increases the crystalline nature in the sample and results in increased intensity of XRD peaks. Intensity of (220) decreases and (311) increases with the incorporation of nickel content. The decrease in the intensity of (220) peak may be the replacement of Fe²⁺, Fe³⁺, instead of Ni²⁺ ion in octahedral site.



(b)

Figure 3.2 (a) XRD pattern of honey-mediated Cu_{1-x}Ni_xFe₂O₄ (x = 0, 0.5, 1.0) nanoparticles and (b) magnified XRD pattern between 35.6° and 37.1°

Figure 3.2(b) shows peak intensity corresponding to (311) plane with Ni content for angle between 35.6° and 37.1°. The shift of XRD peaks towards lower side with nickel ion implies change in lattice parameter. This because of the ionic radius difference of Cu²⁺ (0.73Å) and Ni²⁺ (0.69Å). The variation of lattice constant indicates distribution of divalent nickel ions in B sites. Moreover,

$$a = d\sqrt{h^2 + k^2 + l^2} \quad (3.1)$$

$$D = (0.9\lambda) / (\beta \cos\theta) \quad (3.2)$$

$$dx = (8M) / (Na^3) \quad (3.3)$$

Table 3.1 Crystallite size, lattice parameter, cation distribution, and energy gap of the honey-mediated $\text{Cu}_{1-x}\text{Ni}_x\text{Fe}_2\text{O}_4$ ferrite nanoparticles

| Sample | D (nm) | Lattice Parameter (Å) | X-ray Density (gm/cm ³) | Cation Distribution | Energy gap (eV) |
|--------|--------|-----------------------|-------------------------------------|---|-----------------|
| CuF | 59.15 | 8.250 | 5.662 | $(\text{Fe}^{3+})_{1.0}^{\text{tet}} [\text{Cu}^{2+}, \text{Fe}^{3+}]_{1.0}^{\text{oct}}$ | 1.65 |
| CuNiF | 35.45 | 8.336 | 5.496 | $(\text{Cu}^{2+}\text{Fe}^{3+})_{0.5}^{\text{tet}} [\text{Ni}^{2+}\text{Fe}^{3+}]_{0.5}^{\text{oct}}$ | 1.73 |
| NiF | 44.33 | 8.306 | 5.433 | $(\text{Fe}^{3+})_{1.0}^{\text{tet}} [\text{Ni}^{2+}, \text{Fe}^{3+}]_{1.0}^{\text{oct}}$ | 1.67 |

From the results, it is found that the average crystallite size of the samples depends on the Ni substitution. CuF has 59.15 nm crystallite size; CuNiF ferrite has the lowest crystallite size (35.45 nm); and NiF has 44.33 nm crystallite size. The substitution of nickel reduces the size of the crystallite and obeys the law of Vegard (Sridhar *et al.* 2012).

FTIR Analysis

FTIR spectra of honey-mediated $\text{Cu}_{1-x}\text{Ni}_x\text{Fe}_2\text{O}_4$ ferrite samples from the of 4000–400 cm^{-1} are shown in Figure 3.4. The FTIR spectra helps in the case of ferrites now not only to interpret the structure, but additionally to redistribute. The two fundamental bands of metal oxygen bonds have been observed. The higher frequency band in the range of 600-500 cm^{-1} suggests intrinsic stretching vibrations of tetrahedral complexes whereas the lower frequency band in the range of 450 – 385 cm^{-1} corresponds to octahedral metal complexes (Sertkol *et al.* 2009). In the tetrahedral M-O vibration happens at 581 cm^{-1} . Similarly the octahedral M-O vibration occurs at 412 cm^{-1} . The difference in the band position is anticipated due to the fact of the difference in Fe^{3+} - O^{2-} distance for the octahedral and tetrahedral sites (Nejati *et al.* 2012). The FTIR band at 1378 cm^{-1} is due to stretching vibration of C-H bond of the honey, which is used as a reducing agent (Faghihzadeh *et al.* 2016).

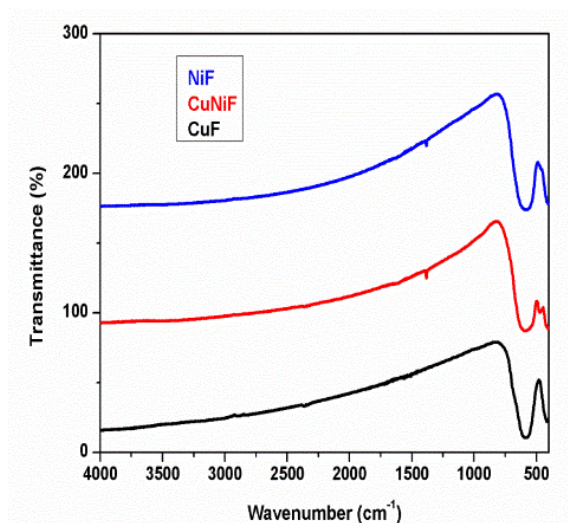


Figure 3.4 FTIR spectrum of honey-mediated $\text{Cu}_{1-x}\text{Ni}_x\text{Fe}_2\text{O}_4$ ($x = 0, 0.5, 1.0$) nanoparticles

Morphological Studies

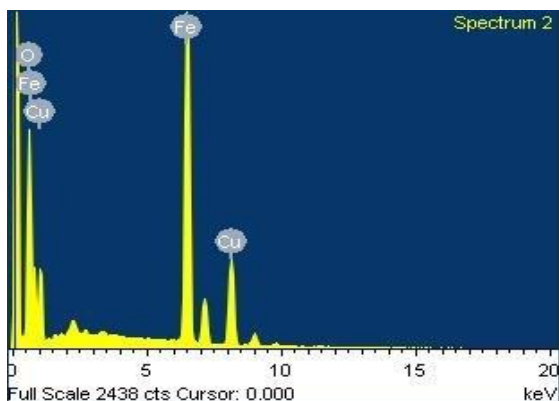
SEM analysis

The morphology of prepared materials are studied using SEM images. Figures 3.5 (a-c) exhibit the scanning electron microscope (SEM) like nanoparticles with agglomeration in nature. The variation of grain size of the SEM images for different samples may also be due to agglomeration caused by way of the magnetic nature of the samples.

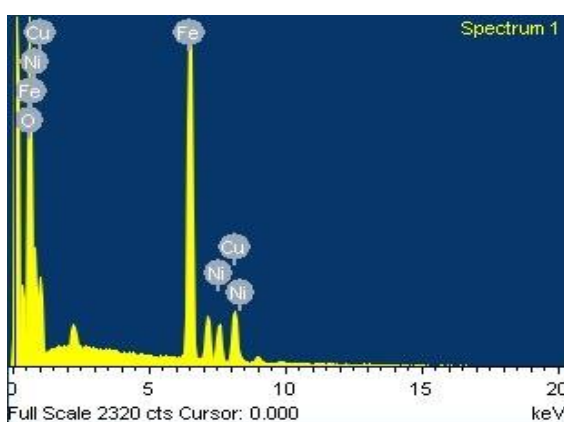
EDX Analysis

Figures 3.6 show the EDX spectra of honey-mediated (a) CuF, (b) CuNiF (c) NiF ferrite nanoparticles. From the pattern indicates the peaks of Fe, Cu, Ni and O. The absence of peaks of any other element, establishes the purity of the sample and no other impurities which confirms the formation of mixed ferrite nanoparticles. The presence of wt % of Fe, Ni, Cu and O factors in the EDX spectra suggested that the molar ratio for Cu/Ni:Fe:O is all close to 0.5:0.5:2:4.

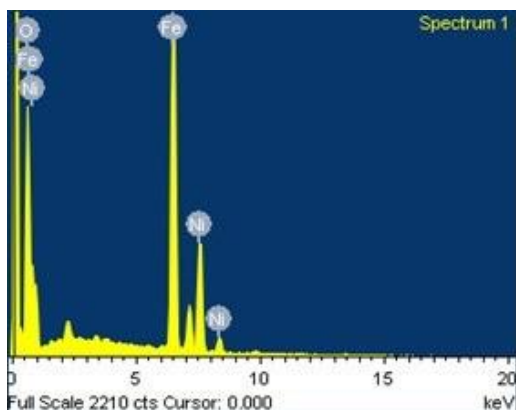
Research Paper



| Elements | Weight% | Atomic% |
|----------|---------|---------|
| O | 24.19 | 53.75 |
| Fe | 49.69 | 31.63 |
| Cu | 26.12 | 14.62 |



| Elements | Atomic Wt% | Weight Wt% |
|----------|------------|------------|
| Cu | 14.10 | 26.87 |
| Ni | 12.31 | 20.90 |
| Fe | 28.36 | 35.25 |
| O | 45.23 | 16.98 |



| Elements | Weight% | Atomic% |
|----------|---------|---------|
| O | 25.78 | 55.22 |
| Fe | 48.57 | 59.81 |
| Ni | 25.65 | 14.97 |

Figure 3.6 EDX spectrum of honey-mediated (a) CuF, (b) CuNiF, (c) NiF nanoparticles

HRTEM analysis

Figure 3.7(a, b) shows the distribution of CuNiFnanoparticles by means of microstructure and particle size. Most of the particles in the TEM images

Research Paper

are seen in spherical shapes, ranging from 30 to 40 nm. Due to the congregation of nanoparticles, darkish areas are recognized in TEM micrograph regions. This takes place due to the fact of the dipolar magnetic nanoparticles, excessive surface area, energy, and interactions.

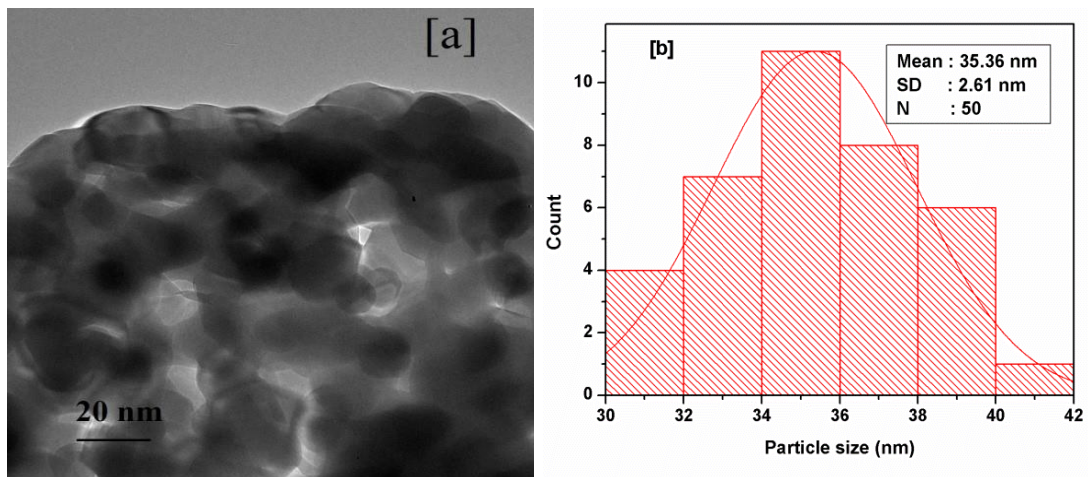


Figure 3.7 (a) HR-TEM image (b) Particle size distribution of honey-mediated CuNiF nanoparticles

SAED pattern

Figure 3.8 represents the Selected Area Electron Diffraction (SAED) patterns for the CuNiF ferrite nanoparticles and the result appears as concentric rings in regular lattice line, that suggests the high crystallinity face founded cubic spinel structure and the presence of nanosized crystals (Sagayaraj *et al.* 2018).

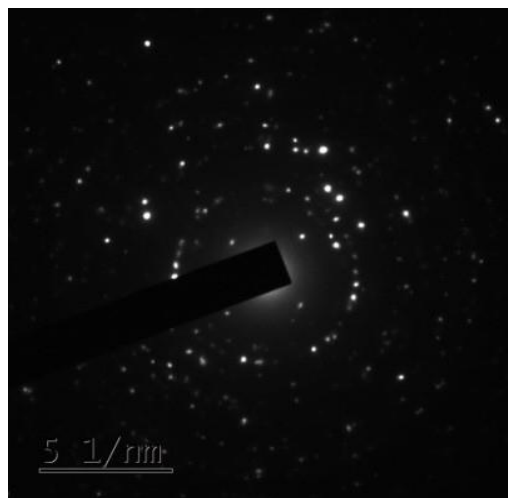


Figure 3.8 SAED pattern of honey-mediated CuNiF ferrite nanoparticles

Optical Properties

UV-visible analysis

The UV-Visible spectrum of the honey-mediated $\text{Cu}_{1-x}\text{Ni}_x\text{Fe}_2\text{O}_4$ ($x = 0.0, 0.5, 1.0$) nanoparticles are shown in Figure 3.9. The band gap energy can be approximately calculated by using the following equation :

$$(\alpha h\nu)^n = A (h\nu - E_g) \quad (3.4)$$

There is no significant variation of the bandgap value with the substitution of Ni content. The value of synthesized ferrite nanoparticles is lower than the value of bulk CuF around 1.92 eV. Various factors such as particle size, morphological parameters and impurity presence, influences the band gap. The attribute worth mentioning is the relationship between bandgap and particle size (Vinosha *et al.* 2008).

Photoluminescence analysis

$\text{Cu}_{1-x}\text{Ni}_x\text{Fe}_2\text{O}_4$ nanoparticles showed peaks corresponding to UV emissions at 380 nm that corresponds to near band edge emission, which is preferable to the exciton-related transitions. Oxygen vacancies can be ascribed to the peak at 520 nm, resulting in green emissions. The slight decrease in green emission intensity (520 nm) with Ni^{2+} content and a decrease in crystallite size indicate different structural defects (Lu *et al.* 2006). It may be due to the decreasing amount of optically active defects as well as heat quenching, because the increase in nonradioactive transition centers is caused by the inclusion of Ni^{2+} and inherent defects such as oxygen deficiency or interstitial-associated defects. It was found that in all

the samples there was no change in the PL peak positions for all green reducing agent-mediated $\text{Cu}_{1-x}\text{Ni}_x\text{Fe}_2\text{O}_4$ nanoparticles except aloe vera extract-mediated ferrite nanoparticles. In the aloe vera-mediated process, PL intensity of CuNiF nanoparticles showed a shift in peak position toward lowerwavelength.

Magnetic Properties

In the case of nickel-substituted copper ferrite nanoparticles, the values of saturation magnetization and remanent magnetization (M_r) increase and the value of coercivity (H_c) decreases with nickel substitution for all green reducing agent-mediated processes except egg white- and sugarcane juice-mediated processes. In egg white-mediated process, the coercivity value slightly increased from 425.41 to 437.36 Oe. However, in the sugarcane- mediated process, it increased from 429.75 to 981.98 Oe and the saturation magnetization vale reduced from 15.40 to 12.6 emu/g.

Antibacterial Activity

The synthesized ferrite nanoparticles showed excellent antimicrobial activity against gram-positive bacteria such as *S. aureus* and *B. subtilis* and against gram-negative bacteria such as *E. coli* and *K. pneumonia*. This was confirmed by the formation of the zones of inhibition with the bacterial growth on the petri plates by agar diffusion method. Sugarcane juice-mediated ferrite nanoparticles showed good antibacterial activity compared with other samples (above 10 mm).

$\text{Cu}_{1-x}\text{Ni}_x\text{Fe}_2\text{O}_4$ nanoparticles were prepared by five green fuels. Among the three fuels, aloe vera extract is a good fuel for the combustion reaction when compared to other fuels.

$\text{Cu}_{1-x}\text{Ni}_x\text{Fe}_2\text{O}_4$ nanoparticles prepared by using aloe vera extract as a fuel has some unique properties. For example, it has less particle size, more of energy bandgap, and better saturation magnetization and coercivity value when compared to other fuels.

The results of this study indicate that the synthesized ferrite nanoparticles developed by the sol–gel method using aloe vera extract as fuel can be found to be economical and most effective, and that they can be a potential material for optoelectromagnetic applications.

FUTURE SCOPE

The work presented in this thesis can be extended in several directions and the scopes of this work are briefly described below:

Mossbauer analysis of the samples can be done to get a clearer picture of cationic distribution over A and B sites with different nickel concentration.

The magnetic measurements at low/high temperature for nickel-substituted copper ferrite nanoparticles can be studied and the corresponding blocking/Curie temperature can be determined.

The oxidation state of the elements of all the samples can be studied by using XPS.

Nanocrystalline ferrites are extensively used as gas and humidity sensors. The sensitivity of nickel-substituted copper ferrites can be checked against various poisonous gases.

Nickel-substituted copper ferrite show good antimicrobial activity. Antimicrobial activity of the nickel-substituted copper ferrite can be investigated against various microbes and fungi.

Ferrite nanoparticles are reported to show good catalytic activity. The catalytic activity of undoped and doped copper ferrite nanoparticles can be analyzed.

REFERENCES

1. Abeyrathne, EDNS, Lee, HY & Ahn, DU 2013, 'Egg white proteins and their potential use in food processing or as nutraceutical and pharmaceutical agents—A review', *Poultry Science*, vol. 92, no. 12, pp. 3292-3299.
2. Agouriane, E, Rabi, B, Essoumhi, A, Razouk, A, Sahlaoui, M, Costa, B F O & Sajieddine, M, 2016, 'Structural and magnetic properties of CuFe₂O₄ ferrite nanoparticles synthesized by co-precipitation', *Journal of Materials and Environmental Science*, vol. 7, no. 11, pp. 4116-4120.

3. Ahamad, HS, Meshram, NS, Bankar, SB, Dhoble, SJ & Rewatkar, KG 2017, 'Structural properties of $\text{Cu}_x\text{Ni}_{1-x}\text{Fe}_2\text{O}_4$ nano. ferrites prepared by urea-gel microwave auto combustion method', *Ferroelectrics*, vol. 516, no. 1, pp. 67-73.
4. Ahmad, B, Mahmood, A, Ashiq, MN, Malana, MA, Najam-Ul-Haq, M, Ehsan, M F & Shakir, I, 2014, 'New multiferroics $\text{BiFe}_{1-2x}\text{Al}_x\text{Mn}_x\text{O}_3$ nanoparticles: Synthesis and evaluation of various structural, physical, electrical, dielectric and magnetic parameters', *Journal of Alloys and Compounds*, vol. 590, pp. 193-198.
5. Ahmed, M A, Rady, K E S, El-Shokrofy, K M, Arais, A A & Shams, M S, 2014, 'The Influence of Zn^{2+} Ions Substitution on the Microstructure and Transport Properties of Mn-Zn Nanoferrites', *Materials Sciences and Applications*, vol. 5, no. 13, pp. 932
6. Akhter, S, Paul, D P, Hakim, M A, Saha, D K, Al-Mamun, M & Parveen, A 2011, 'Synthesis, structural and physical properties of $\text{Cu}_{1-x}\text{Zn}_x\text{Fe}_2\text{O}_4$ ferrites', *Materials Sciences and Applications*, vol. 2, no. 11, pp. 1675.
7. Akinyele, B O & Odiyi, A C 2007, 'Comparative study of vegetative morphology and the existing taxonomic, nutritional and medicinal status of Aloe vera L', In 8th African Crop Science Society Conference, El-Minia, Egypt, 27-31 October 2007, African Crop Science Society, pp. 1567-1570.
8. Alahmadi, N S, Betts, J W, Cheng, F, Francesconi, M G, Kelly, S M, Kornherr, A & Wadhawan, J D 2017, 'Synthesis and antibacterial effects of cobalt-cellulose magnetic nanocomposites', *RSC Advances*, vol. 7, no. 32, pp. 20020-20026.
9. Ali, A, Zafar, H, Zia, M, ul Haq, I, Phull, A R, Ali, J S & Hussain, A 2016, 'Synthesis, characterization, applications, and challenges of iron oxide nanoparticles Nanotechnology', *Science and Applications Dove Medical Press Ltd* <https://doi.org/102147/NSAS99986>.
10. Amir, M, Baykal, A, Güner, S, Sertkol, M, Sözeri, H & Toprak, M 2015, 'Synthesis and Characterization of $\text{Co}_x\text{Zn}_{1-x}\text{AlFeO}_4$ Nanoparticles Journal of Inorganic and Organometallic', *Polymers and Materials*, vol. 25, no. 4, pp. 747-754.
11. Amiri, S & Shokrollahi, H 2013, 'The role of cobalt ferrite magnetic nanoparticles in medical science', *Materials Science and Engineering C* <https://doi.org/101016/jmse201209003>.
12. Angeline Mary, A P, Thaminum Ansari, A & Subramanian, R 2019, 'Sugarcane juice mediated synthesis of copper oxide nanoparticles, characterization and their antibacterial activity', *Journal of King Saud University - Science* <https://doi.org/101016/jjksus201903003>
13. Anjana, V, John, S, Prakash, P, Nair, A M, Nair, A R, Sambhudevan, S & Shankar, B, 2018, 'Magnetic properties of copper doped nickel ferrite nanoparticles synthesized by Co precipitation method In IOP Conference Series', *Materials Science and Engineering*, IOP Publishing, vol. 310, no. 1, p 012024.
14. Anjum, S, Saleem, H, Rasheed, K, Zia, R, Riaz, S & Usman, A, 2017, 'Role of Ni^{2+} ions in magnetite nano-particles synthesized by Co- precipitation

Research Paper

- method', *Journal of Superconductivity and Novel Magnetism*, vol. 30, no. 5, pp. 1177-1186.
15. Ati, A A 2018, 'Fast synthesis, structural, morphology with enhanced magnetic properties of cobalt doped nickel ferrite nanoscale', *Journal of Materials Science: Materials in Electronics*, vol. 29, no. 14, pp. 12010-12021.
16. Aziz, H S, Rasheed, S, Khan, R A, Rahim, A, Nisar, J, Shah, S M, ... & Khan, A R, 2016, 'Evaluation of electrical, dielectric and magnetic characteristics of Al-La doped nickel spinel ferrites', *RSC Advances*, vol. 6, no. 8, pp. 6589-6597 <https://doi.org/10.1039/c5ra20981a>.
17. Babukutty, B, Kalarikkal, N & Nair, S S 2017, 'Studies on structural, optical and magnetic properties of cobalt substituted magnetite fluids ($\text{Co}_x\text{Fe}_{1-x}\text{Fe}_2\text{O}_4$)', *Materials Research Express*, vol. 4, no. 3 <https://doi.org/10.1088/2053-1591/aa628b>
18. Balavijayalakshmi, J, Suriyanarayanan, N & Jayaprakash, R, 2015, 'Role of copper on structural, magnetic and dielectric properties of nickel ferrite nano. Particles', *Journal of Magnetism and Magnetic Materials*, vol. 385, pp. 302-307 <https://doi.org/10.1016/j.jmmm.2015.03.036>
19. Bammannavar, B K, Naik, L R, Pujar, R B & Chougule, B K 2008, 'Influence of Time and Temperature on Resistivity and Microstructure of $\text{Cu}_x\text{Co}_{1-x}\text{Fe}_2\text{O}_4$ Mixed Ferrites Progress', In *Electromagnetics Research*, vol. 4, pp. 121-129
20. Basu, S, Hossain, S K M, Chakravorty, D & Pal, M 2011, 'Enhanced magnetic properties in hydrothermally synthesized Mn-doped BiFeO_3 nanoparticles', *Current Applied Physics*, vol. 11, no. 4, pp. 976-980
21. Battle, X & Labarta, A 2002, 'Finite-size effects in fine particles: Magnetic and transport properties', *Journal of Physics D: Applied Physics* <https://doi.org/10.1088/0022-3727/35/6/201>
22. Birajdar, A A, Shirsath, S E, Kadam, R H, Patange, S M, Mane, D R & Shitre, A R 2012, 'Rietveld Structure Refinement and Cation Distribution of Substituted Nanocrystalline Ni-Zn Ferrites', *ISRN Ceramics*, pp. 1-5 <https://doi.org/10.5402/2012/876123>
23. Bogdanov, S, Jurendic, T, Sieber, R & Gallmann, P, 2008, 'Honey for nutrition and health: a review', *Journal of the American College of Nutrition*, vol. 27, no. 6, pp. 677-689.
24. Bradford, P, 2001, 'The aggregation of iron oxide nanoparticles in magnetic fields', vol. 91, pp. 29-32.
25. Brundle, C R, Evans, C A & Wilson, S 1992, 'Encyclopedia of materials characterization: surfaces, interfaces, thin films', GulfProfessional Publishing.
26. Carp, O, Huisman, C L & Reller, A, 2004, 'Photoinduced reactivity of titanium dioxide', *Progress in Solid State Chemistry*, vol. 32, no. 1-2, pp. 33-177.
27. Chatterjee, B K, Bhattacharjee, K, Dey, A, Ghosh, C K & Chattopadhyay, K K, 2014, 'Influence of spherical assembly of copper ferrite nanoparticles on magnetic properties: orientation of magnetic easy axis', *Dalton Transactions*, vol. 43, no. 21, pp. 7930-7944

28. Ciciliati, M A, Silva, M F, Fernandes, D M, de Melo, M A, Hechenleitner, A A W & Pineda, E A 2015, 'Fe-doped ZnO nanoparticles: Synthesis by a modified sol-gel method and characterization', *Materials Letters*, vol. 159, pp. 84-86.
29. Cruz, D M, Tien-Street, W, Zhang, B, Huang, X, Crua, A V, Nieto-Argüello, A & García-Martín, J M 2019, 'Citric juice-mediated synthesis of tellurium nanoparticles with antimicrobial and anticancer properties', *Green Chemistry*, vol. 21, no. 8, pp. 1982-1998.
30. Cullity, B D & Graham, C D 2009, 'Appendix 2: Data on Ferromagnetic Elements In Introduction to Magnetic Materials', John Wiley & Sons, Inc, pp. 531-531 <https://doi.org/10.1002/9780470386323>
31. Cullity, B D & Stock, S R 2001, 'Elements of X-ray Diffraction', New Jersey: Prentice Hall, vol. 3, p. 15.
32. Dar, M A, Majid, K, Najar, M H, Kotnala, R K, Shah, J, Dhawan, S K & Farukh, M 2017, 'Surfactant-assisted synthesis of polythiophene/ Ni_{0.5}Zn_{0.5}Fe_{2-x}Ce_xO₄ ferrite composites: study of structural, dielectric and magnetic properties for EMI-shielding applications', *Physical Chemistry Chemical Physics*, vol. 19, no. 16, pp. 10629-10643.
33. Dasan, Y K, Guan, B H, Zahari, M H & Chuan, L K 2017, 'Influence of La³⁺ substitution on structure, morphology and magnetic properties of nanocrystalline Ni-Zn ferrite', *PLoS ONE*, vol. 12, no. 1, <https://doi.org/10.1371/journal.pone.0170075>